Generating Schrödinger-cat-like states by means of conditional measurements on a beam splitter

M. Dakna, T. Anhut, T. Opatrný,* L. Knöll, and D.-G. Welsch

Friedrich-Schiller-Universität Jena, Theoretisch-Physikalisches Institut, Max-Wien-Platz 1, D-07743 Jena, Germany

(Received 2 December 1996)

A scheme for generating Schrödinger-cat-like states of a single-mode optical field by means of conditional measurement is proposed. Feeding a squeezed vacuum into a beam splitter and counting the photons in one of the output channels, the conditional states in the other output channel exhibit a number of properties that are very similar to those of superpositions of two coherent states with opposite phases. We present analytical and numerical results for the photon-number and quadrature-component distributions of the conditional states and their Wigner and Husimi functions. Further, we discuss the effect of realistic photocounting on the states. [S1050-2947(97)06404-4]

PACS number(s): 42.50.Dv, 03.65.Bz

I. INTRODUCTION

It is well known that according to the basic-theoretical principles of quantum-mechanics, the superposition of macroscopically distinguishable quantum states can give rise to quantum interferences such that the resulting states are highly nonclassical. Schrödinger [1] illustrated this phenomenon by a gedankenexperiment to get a cat into a superposition of a live and a dead cat. A number of systems have been studied with the aim of the realization of Schrödinger-cat-like states, where the ''cat'' is typically a mesoscopic system that has both microscopic and macroscopic (i.e., classically distinguishable) properties.

In harmonic oscillators, typical examples of Schrödinger-cat-like states are superpositions of two coherent (i.e., most classical) states with opposite phases [2]. The superposition states exhibit some properties similar to those of simple statistical mixtures, but they also reveal typical interference features. Measuring the quadrature-component distribution, one observes two peaks that change their mutual distance in dependence on the phase of the quadrature component until they eventually overlap. In this particular case the difference between a coherent superposition and a statistical mixture is the most distinct. Whereas in the former case quantum interferences are observed which give rise to an oscillatory behavior of the quadrature-component distribution, in the latter case a single peak without interference structure is observed. The creation of such states in realistic experiments is not trivial. Proposals for preparing vibrations in molecules or crystals in Schrödinger-cat-like states have been made [3,4]. Recently, it has been proposed that Schrödinger-cat-like states of a single harmonically bound (trapped) atom can be produced by appropriately driving the atom [5], and experiments have successfully been performed [6]. The possibility of preparing a harmonically bound atom in a superposition of two coherent squeezed states with opposite phases has also been studied [7].

Several proposals have been made to prepare a single-mode radiation field (which also corresponds to a harmonic oscillator) in a Schrödinger-cat-like state (see, e.g., [8] and references therein). In particular, it has been proposed that conditional measurements may be used advantageously to realize such states. It is well known that if a quantity of a subsystem of a correlated two-part system prepared in some entangled state is measured, the state of the other subsystem ''collapses'' to a particular state. To produce conditional states of the type of Schrödinger-cat-like states, the use of a scheme for optical back-action-evading measurement in nonlinear media [9] was suggested [10]. The calculations show that when the photon number of the readout mode is measured, then a superposition of macroscopically distinguishable quantum states is generated in the signal mode [10]. To improve the scheme, it was proposed that a squeezed vacuum at the signal frequency is injected instead of amplifying the signal after back-action-evading measurement [11]. Recently, a modification of this scheme was studied, with special emphasis on the experimental feasibilities with current technologies [12,13].

In this paper we show that Schrödinger-cat-like states can already be obtained using a simple beam-splitter scheme for a conditional measurement of the type considered recently in [14,15]. The calculations show that when a squeezed vacuum is injected in one of the input channels (the second input channel being unused) and the photon number of the mode in one of the output channels is measured, then the mode in the other output channel is prepared in a conditional state that has the typical features of a Schrödinger-cat-like state. In particular, the conditional states can be regarded as superpositions of two quantum states that are well localized in the phase space and bear a strong resemblance to squeezed coherent states. To demonstrate this, we analyze the states in terms of the photon-number and quadrature-component distributions and the Wigner and Husimi functions. We further discuss possible modifications of the states in realistic multichannel photon detection.

The paper is organized as follows. In Sec. II the conditional states are derived, and in Sec. III their properties are discussed. Section IV is devoted to a realistic detection scheme. Finally, a summary and some concluding remarks are given in Sec. V.

---
*Permanent address: Palacký University, Faculty of Natural Sciences, Svobody 26, 77146 Olomouc, Czech Republic.

II. BASIS EQUATIONS

Let us consider a lossless beam splitter and assume that the input fields can be regarded as being effectively single mode fields, with photon destruction and creation operators $\hat{a}_k$ and $\hat{a}_k^\dagger$, respectively ($k = 1,2$). The photon destruction and creation operators of the output modes $\hat{b}_k$ and $\hat{b}_k^\dagger$, respectively, can then be obtained using the well-known input-output relations

$$\hat{b}_k = \sum_{k'=1}^{2} T_{k,k'} \hat{a}_{k'}, \tag{1}$$

where

$$(T_{k,k'}) = e^{i\varphi_0} \begin{pmatrix} \cos\theta e^{i\varphi_T} & \sin\theta e^{i\varphi_R} \\ -\sin\theta e^{-i\varphi_R} & \cos\theta e^{-i\varphi_T} \end{pmatrix} \tag{2}$$

is a SU(2) matrix whose elements are given by the complex transmittances and reflectances of the beam splitter from the two sides. Equation (1) corresponds to a unitary transformation of the operators in the Heisenberg picture, $\hat{b}_k = \hat{V} \hat{a}_k \hat{V}^\dagger$ ($k = 1,2$). Equivalently, the Schrödinger picture can be used, in which the photonic operators are left unchanged and the density operator is transformed such that the output-state density operator $\hat{\varrho}_{\text{out}}$ is obtained from the input-state density operator $\hat{\varrho}_{\text{in}}$ as

$$\hat{\varrho}_{\text{out}} = \hat{V}^\dagger \hat{\varrho}_{\text{in}} \hat{V}. \tag{3}$$

The operator $\hat{V}$ can be given by [16,17]

$$\hat{V} = e^{-i(\varphi_T - \varphi_R)\hat{L}_3} e^{-2i\theta\hat{L}_2} e^{-i(\varphi_T + \varphi_R)\hat{L}_3}, \tag{4}$$

where

$$\hat{L}_2 = \frac{1}{2i}(\hat{a}_1^\dagger \hat{a}_2 - \hat{a}_2^\dagger \hat{a}_1), \quad \hat{L}_3 = \frac{1}{2}(\hat{a}_1^\dagger \hat{a}_1 - \hat{a}_2^\dagger \hat{a}_2), \tag{5}$$

and $\varphi_0 = 0$ (note that φ_0 is a global phase factor that may be omitted without loss of generality).

Now, let us assume that the mode in the first input channel is prepared in a state described by a density operator $\hat{\varrho}_{\text{in1}}$ and the second channel is unused, so that the input-state density operator reads as

$$\hat{\varrho}_{\text{in}} = \hat{\varrho}_{\text{in1}} \otimes |\text{vac}_2\rangle\langle\text{vac}_2|. \tag{6}$$

Using Eqs. (4) and (6), the output-state density operator (3) can be given by [14,15]

$$\hat{\varrho}_{\text{out}} = \sum_{n_2=0}^{\infty} \sum_{m_2=0}^{\infty} \left\{ \frac{e^{-i(m_2-n_2)\varphi_R}}{\sqrt{m_2! n_2!}} (-1)^{m_2+n_2} \left| \frac{R}{T} \right|^{m_2+n_2} \right.$$
$$\times e^{i\varphi_T \hat{a}_1^\dagger \hat{a}_1} \hat{a}_1^{m_2} |T|^{\hat{a}_1^\dagger \hat{a}_1} \hat{\varrho}_{\text{in1}} |T|^{\hat{a}_1^\dagger \hat{a}_1} (\hat{a}_1^\dagger)^{n_2}$$
$$\left. \times e^{-i\varphi_T \hat{a}_1^\dagger \hat{a}_1} \otimes |m_2\rangle\langle n_2| \right\}, \tag{7}$$

where $|T| = \cos\theta$ and $|R| = \sin\theta$, and $|n_k\rangle$ are the eigenstates of the photon-number operators $\hat{a}_k^\dagger \hat{a}_k$. From Eq. (7) we see that the output modes are, in general, highly correlated.

When the photon number of the mode in the second output channel is measured and m_2 photons are detected, then the mode in the first output channel is prepared in a quantum state whose density operator $\hat{\varrho}_{\text{out1}}$ reads as

$$\hat{\varrho}_{\text{out1}}(m_2) = \frac{\langle m_2 | \hat{\varrho}_{\text{out}} | m_2 \rangle}{\text{Tr}_1(\langle m_2 | \hat{\varrho}_{\text{out}} | m_2 \rangle)}. \tag{8}$$

The probability of such an event is given by

$$P(m_2) = \text{Tr}_1(\langle m_2 | \hat{\varrho}_{\text{out}} | m_2 \rangle)$$
$$= \sum_{n_1=m_2}^{\infty} \binom{n_1}{m_2} (1-|T|^2)^{m_2} |T|^{2(n_1-m_2)} \langle n_1 | \hat{\varrho}_{\text{in1}} | n_1 \rangle. \tag{9}$$

In particular, if the first input mode is prepared in a squeezed vacuum state, we may write

$$\hat{\varrho}_{\text{in1}} = \hat{S}(\xi) |\text{vac}_1\rangle\langle\text{vac}_1| \hat{S}^\dagger(\xi), \tag{10}$$

where

$$\hat{S}(\xi)|\text{vac}_1\rangle = \exp\left\{ -\frac{1}{2} [\xi(\hat{a}_1^\dagger)^2 - \xi^* \hat{a}_1^2] \right\} |\text{vac}_1\rangle$$
$$= (1-|\kappa|^2)^{1/4} \sum_{n_1=0}^{\infty} \frac{[(2n_1)!]^{1/2}}{2^{n_1} n_1!} \kappa^{n_1} |2n_1\rangle, \tag{11}$$

$\xi = |\xi| e^{i\varphi_\xi}$, $\kappa = e^{i\varphi_\xi} \tanh|\xi|$. Combining Eqs. (7) and (8) and using Eqs. (6), (10), and (11), we derive that

$$\hat{\varrho}_{\text{out1}}(m_2) = |\Psi_{m_2}\rangle\langle\Psi_{m_2}|, \tag{12}$$

where

$$|\Psi_{m_2}\rangle = |\Psi_{m_2}(\alpha)\rangle = \frac{1}{\sqrt{\mathcal{N}_{m_2}}} \sum_{n_1=0}^{\infty} c_{m_2,n_1}(\alpha) |n_1\rangle, \tag{13}$$

$$c_{m_2,n_1}(\alpha) = \frac{(n_1+m_2)!}{\Gamma[\frac{1}{2}(n_1+m_2)+1]\sqrt{n_1!}}$$
$$\times \frac{1}{2}[1+(-1)^{n_1+m_2}](\frac{1}{2}\alpha)^{(n_1+m_2)/2}, \tag{14}$$

$\alpha = |\alpha| e^{i\varphi_\alpha}$, with $|\alpha| = |T|^2 |\kappa|$ and $\varphi_\alpha = 2\varphi_T + \varphi_\xi$. In what follows we will restrict attention to real values of α ($-1 \leq \alpha \leq 1$), i.e., $\varphi_\alpha = 0, \pi$, since from Eqs. (13) and (14) the effect of other phases φ_α is simply a rotation in phase space. Applying the relations (A2), (A3), and (A6) in Appendix A, the normalization constant

$$\mathcal{N}_{m_2} = \sum_{n_1=0}^{\infty} |c_{m_2,n_1}(\alpha)|^2 \tag{15}$$

can be given by

$$\mathcal{N}_{m_2} = \frac{1}{\sqrt{1-\alpha^2}} \left[\frac{\alpha^2}{(1-\alpha^2)} \right]^{m_2}$$

$$\times \sum_{k=0}^{[m_2/2]} \frac{(m_2!)^2}{(m_2-2k)!(k!)^2(2\alpha)^{2k}}, \qquad (16)$$

where the symbol $[x]$ in the summation upper limit denotes the integral part of x. Similarly, using Eqs. (6), (10), and (11) and applying the relations (A2), (A3), and (A6), Eq. (9) yields

$$P(m_2) = \sqrt{\frac{1-\kappa^2}{1-\alpha^2}} \left[\frac{\alpha^2(1-|T|^2)}{|T|^2(1-\alpha^2)} \right]^{m_2}$$

$$\times \sum_{k=0}^{[m_2/2]} \frac{m_2!}{(m_2-2k)!(k!)^2(2\alpha)^{2k}}. \qquad (17)$$

From Eqs. (13) and (14) we easily see that when the detected number of photons in one output channel, m_2, is even (odd), then the mode in the other output channel is prepared in a quantum state $|\Psi_{m_2}\rangle$ that contains only contributions from photon-number states with even (odd) numbers of photons. This property, which gives rise to oscillations in the photon-number distribution of the output state $|\Psi_{m_2}\rangle$, obviously reflects the fact that the squeezed vacuum that is fed in consists of pairs of photons. In particular, when the number of detected photons, m_2, is zero, then the output state is again a squeezed vacuum, but with the parameter α in place of κ.

III. PROPERTIES OF THE CONDITIONAL STATES

To study the properties of the conditional states $|\Psi_m\rangle = |\Psi_m(\alpha)\rangle$ in more detail, we will calculate the photon-number and quadrature-component distributions and the Wigner and Husimi functions. Further, we will show that the states $|\Psi_m\rangle$ can be represented as superpositions of two macroscopically distinguishable ''quasicoherent'' squeezed states. For notational convenience we will omit the subscripts 1 and 2 introduced above to distinguish between the two output channels.

A. Photon-number distribution

Recalling Eq. (13), the photon-number distribution

$$P(n|m) = |\langle n|\Psi_m\rangle|^2 \qquad (18)$$

of a state $|\Psi_m\rangle$ reads as

$$P(n|m) = \mathcal{N}_m^{-1}|c_{m,n}(\alpha)|^2, \qquad (19)$$

where $c_{m,n}(\alpha)$ and $\mathcal{N}_m$ are given in Eqs. (14) and (15), respectively. In particular, the mean photon number

$$\langle \hat{n} \rangle = \mathcal{N}_m^{-1} \sum_{n=0}^{\infty} n|c_{m,n}(\alpha)|^2 \qquad (20)$$
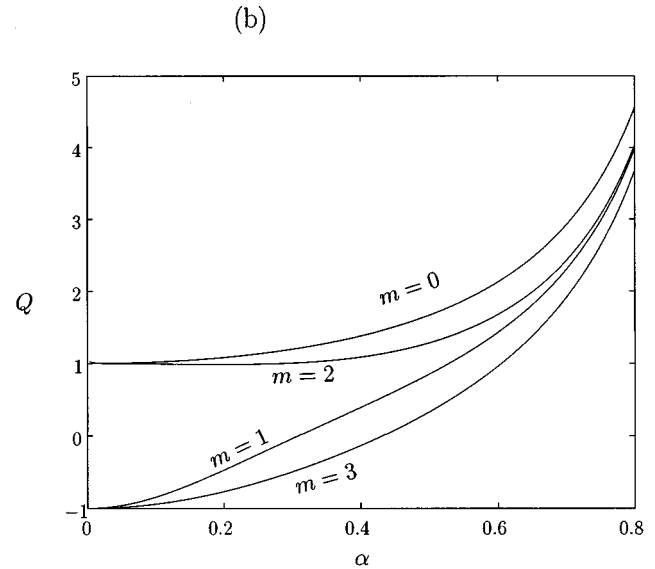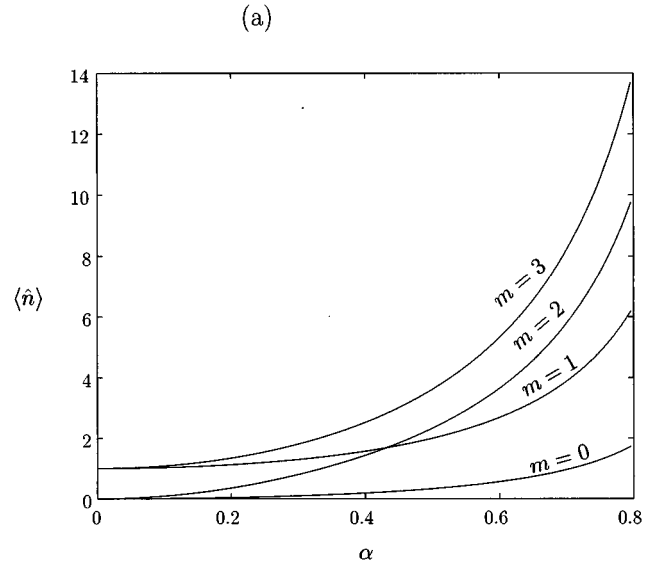
can be given by

FIG. 1. (a) Mean photon number $\langle \hat{n} \rangle$ of the conditional state $|\Psi_m\rangle$ as a function of α for various numbers m of measured photons. (b) Dependence on α of the Mandel Q parameter for the same values of m as in (a).

$$\langle \hat{n} \rangle = \alpha \frac{\partial}{\partial \alpha} \ln \left[\frac{\mathcal{N}_m}{\alpha^m} \right]$$

$$= \frac{\alpha^2}{1-\alpha^2} + m \frac{1+\alpha^2}{1-\alpha^2} - 2 \sum_{k=0}^{[m/2]} k a_{k,m} \left[\sum_{k=0}^{[m/2]} a_{k,m} \right]^{-1}, \qquad (21)$$

where $a_{k,m} = (2\alpha)^{-2k}/[(m-2k)!(k!)^2]$. Examples are shown in Fig. 1(a). We see that the number of photons that can be found in $|\Psi_m\rangle$ increases with m. This is simply a consequence of the beam-splitter transformation. Since one of the input channels is unused, the mean numbers of pho-

tons in the two output channels are proportional to each other, the ratio being given by $|T/R|^2$. Note that when no photons are detected, $m=0$, then $\langle\hat{n}\rangle$ reduces to the mean number of photons of a squeezed vacuum, $\langle\hat{n}\rangle = \alpha^2/(1-\alpha^2)$.

A measure of the deviation of the photon-number distribution from a Poissonian is the Mandel Q parameter [18],

$$Q = \frac{\langle\hat{n}^2\rangle - \langle\hat{n}\rangle^2}{\langle\hat{n}\rangle} - 1, \qquad (22)$$

which can be given by

$$Q = \frac{\alpha^2}{\langle\hat{n}\rangle}\frac{\partial^2}{\partial\alpha^2}\ln\left[\frac{\mathcal{N}_m}{\alpha^m}\right] = \frac{\alpha}{\langle\hat{n}\rangle}\frac{\partial}{\partial\alpha}\langle\hat{n}\rangle - 1. \qquad (23)$$

The dependence on α and m of Q is shown in Fig. 1(b). In particular, for even m we find that $Q>0$ for all values of α, which means that the photon-number statistics of $|\Psi_m\rangle$ is super-Poissonian. For odd m and small values of $|\alpha|$ the statistics becomes sub-Poissonian ($Q<0$). Note that the behavior is typical for Schrödinger-cat-like states [8].

B. Quadrature distributions

In order to calculate the conditional quadrature-component distribution (i.e., the phase-parametrized field-strength distribution)

$$p(x,\varphi|m) = |\langle x,\varphi|\Psi_m\rangle|^2, \qquad (24)$$

which can be measured in balanced homodyne detection, we first expand the eigenvectors $|x,\varphi\rangle$ of the quadrature component

$$\hat{x}(\varphi) = 2^{-1/2}(e^{-i\varphi}\hat{a} + e^{i\varphi}\hat{a}^\dagger) \qquad (25)$$

in the photon-number basis as [19]

$$|x,\varphi\rangle = (\pi)^{-1/4}\exp(-\tfrac{1}{2}x^2)\sum_{n=0}^\infty \frac{e^{in\varphi}}{\sqrt{2^n n!}}\,\mathrm{H}_n(x)|n\rangle \qquad (26)$$

(H_n is the Hermite polynomial). Using Eqs. (13) and (26) and applying the relations (A3) and (A6), the conditional quadrature-component distribution (24) reads

$$p(x,\varphi|m) = \frac{|\alpha|^m}{\mathcal{N}_m\sqrt{\pi\Delta^{m+1}}2^m}\exp\left(-\frac{1-\alpha^2}{\Delta}x^2\right)$$
$$\times |\mathrm{H}_m[\sqrt{(\alpha e^{i2\varphi}-\alpha^2)/\Delta}\; x]|^2, \qquad (27)$$

where the abbreviation

$$\Delta = 1 + \alpha^2 - 2\alpha\cos(2\varphi) \qquad (28)$$

has been used.

From Fig. 2 we see that for φ near $\pi/2$ the quadrature-component distribution $p(x,\varphi|m)$ ($m>0$) exhibits two separated peaks, whereas for φ close to 0 or π an interference pattern is observed. It should be noted that although the quadrature-component distribution (27) bears a strong resemblance to that obtained in Ref. [11], a more detailed comparison shows that they are different. Clearly, the beam-splitter transformation, Eqs. (3)–(5), cannot be identified, in general, with the transformation in the back-action-evading scheme considered in Ref. [11].

C. Wigner function

Using Eqs. (13) and (26) together with the relations (A3) and (A6), the Wigner function $W(x,p|m)$ of the state $|\Psi_m\rangle$,

$$W(x,p|m) = \frac{1}{\pi}\int_{-\infty}^{+\infty} dy\, e^{2ipy}\langle x-y|\Psi_m\rangle\langle\Psi_m|x+y\rangle, \qquad (29)$$

can be calculated in a straightforward way. We obtain

$$W(x,p|m) = \frac{2\alpha^m e^{-\lambda x^2}}{\pi^{3/2}\mathcal{N}_m[2(\alpha+1)]^{m+1}}$$
$$\times \int_{-\infty}^{+\infty} dy\left\{e^{-\lambda y^2 + 2ipy}\mathrm{H}_m\left[i\sqrt{\frac{\alpha}{1+\alpha}}(y-x)\right]\right.$$
$$\left.\times \mathrm{H}_m\left[i\sqrt{\frac{\alpha}{1+\alpha}}(x+y)\right]\right\}, \qquad (30)$$

$$\lambda = \frac{1-\alpha}{1+\alpha}, \qquad (31)$$

which after calculation of the integral [20] can be given by

$$W(x,p|m) = \frac{1}{\pi\mathcal{N}_{1m}}\exp\left(-\lambda x^2 - \frac{p^2}{\lambda}\right)\sum_{k=0}^m \frac{(-2|\alpha|)^k}{k![(m-k)!]^2}$$
$$\times \left|\mathrm{H}_{m-k}\left[i\sqrt{\alpha\lambda}\left(x + i\frac{p}{\lambda}\right)\right]\right|^2, \qquad (32)$$

where

$$\mathcal{N}_{1m} = \sum_{k=0}^{[m/2]} \frac{(2|\alpha|)^{m-2k}}{(m-2k)!(k!)^2}. \qquad (33)$$

Equation (32) reveals that when no photons are detected, $m=0$, then the Wigner function exhibits a single peak and simply corresponds to a squeezed-vacuum Gaussian, as already mentioned in Sec. II. Examples of $W(x,p|m)$ ($m>0$) are shown in Fig. 3. From the plots, two separated peaks and an oscillatory regime between them can be seen—a shape that is typical of Schrödinger-cat-like states. The separation of the two peaks is seen to increase with the number m of detected photons. Since with increasing m the number of photons in the conditional state $|\Psi_m\rangle$ also increases, which is a consequence of the beam-splitter transformation, the behavior is quite similar to that of a superposition of two coherent states.

D. Husimi function

The Husimi function $Q(x,p|m)$ of the state $|\Psi_m\rangle$ is defined by
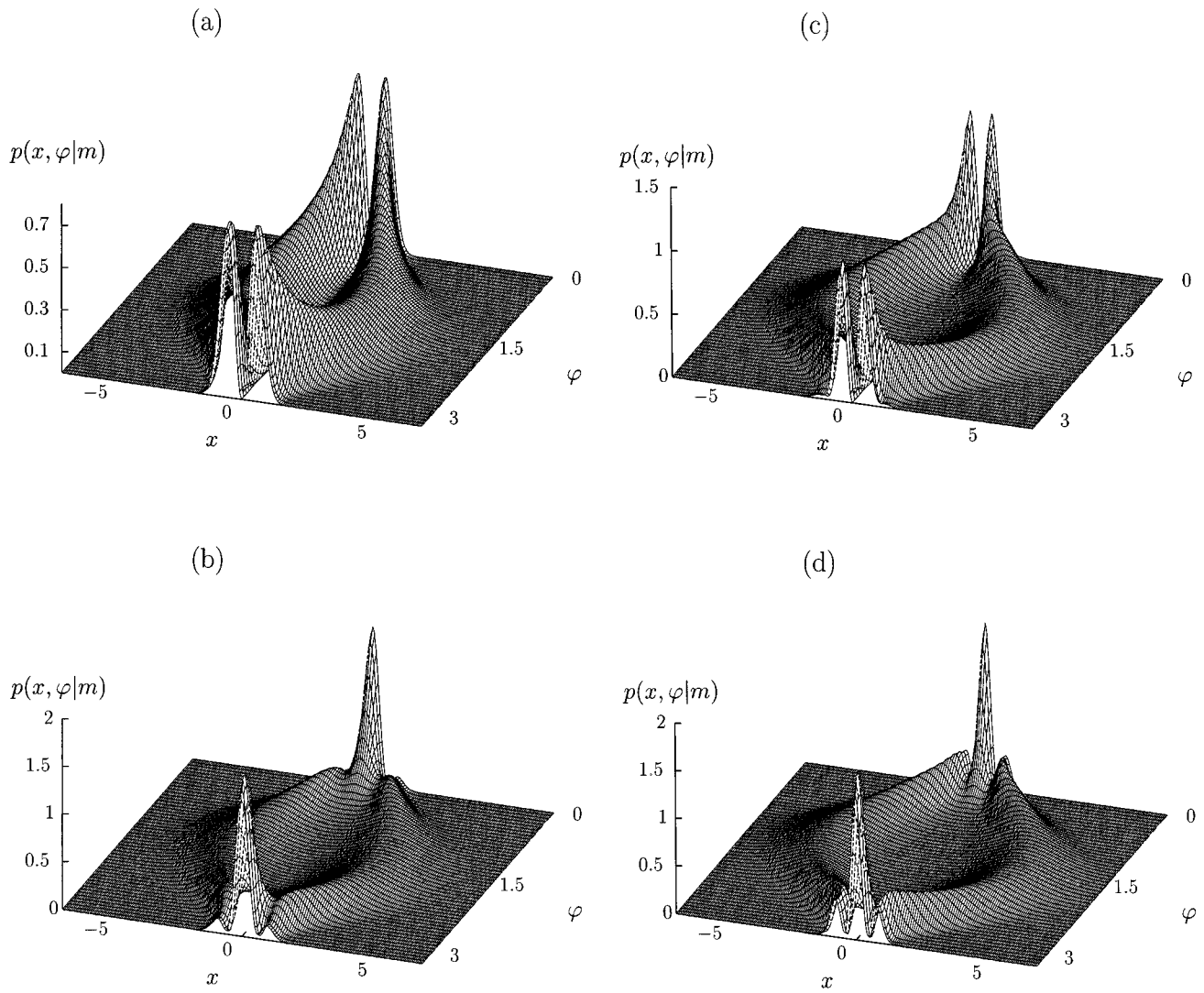
(a)

(c)

(b)

(d)

FIG. 2. Quadrature distribution $p(x,\varphi|m)$ of the conditional state $|\Psi_m\rangle$ for $\alpha=0.6$ and various numbers m of measured photons [(a) $m=1$, (b) $m=2$, (c) $m=3$, (d) $m=4$].

$$Q(x,p|m)=\frac{1}{2\pi}|\langle\beta|\Psi_m\rangle|^2, \qquad (34)$$

where $|\beta\rangle$ is a coherent state and $\beta=2^{-1/2}(x+ip)$. It is worth noting that, contrary to the Wigner function, the Husimi function is a phase-space function that can directly be measured in multiport balanced homodyning using six-port [21,22] or eight-port schemes [23,24]. Expanding $|\beta\rangle$ in the Fock basis,

$$|\beta\rangle=e^{-|\beta|^2/2}\sum_{n=0}^{\infty}\frac{\beta^n}{\sqrt{n!}}|n\rangle, \qquad (35)$$

and recalling Eq. (13) and the relations (A3) and (A7), the scalar product $\langle\beta|\Psi_m\rangle$ can easily be calculated. After some algebra we find that $Q(x,p|m)$ can be written as

$$Q(x,p|m)=\frac{|\alpha|^m}{\pi\mathcal{N}_m 2^{m+1}}\left|H_m\left[\frac{1}{2}i\sqrt{\alpha}(x+ip)\right]\right|^2$$

$$\times\exp\{-\tfrac{1}{2}[(1-\alpha)x^2+(1+\alpha)p^2]\}. \qquad (36)$$

As expected, for $m=0$ the Husimi function is Gaussian, whereas for $m>0$ a two-peak structure is observed. Since the Husimi function is always non-negative, the interference properties of the state are not so apparent as in the case of the Wigner function.

E. Component states

Schrödinger-cat-like states are commonly defined as superpositions of two macroscopically distinguishable quantum states. From Eqs. (13) and (14) it is seen that $|\Psi_m\rangle$ can be regarded as a superposition of states $|\Psi_m^{(+)}\rangle$ and $|\Psi_m^{(-)}\rangle$ as follows:

$$|\Psi_m\rangle=A(|\Psi_m^{(+)}\rangle+|\Psi_m^{(-)}\rangle), \qquad (37)$$

where

$$|\Psi_m^{(\pm)}\rangle=\frac{1}{\sqrt{\mathcal{N}_m^{(\pm)}}}\sum_{n=0}^{\infty}c_{m,n}^{(\pm)}(\alpha)|n\rangle, \qquad (38)$$

with

(a)

$W(x,p|m)$

(c)
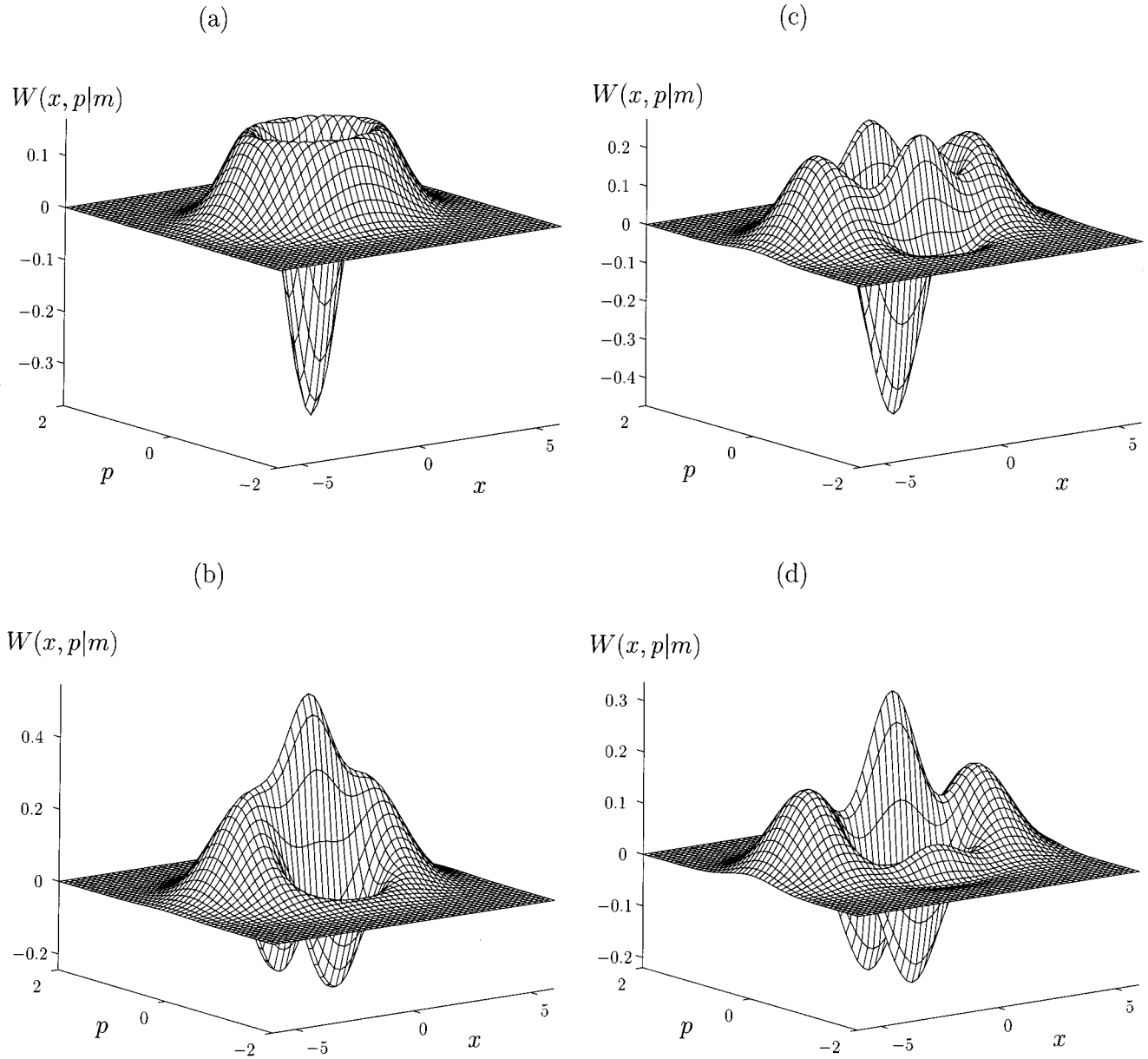
$W(x,p|m)$

(b)

$W(x,p|m)$

(d)

$W(x,p|m)$

FIG. 3. Wigner function $W(x,p|m)$ of the conditional state $|\Psi_m\rangle$ for $\alpha=0.6$ and various numbers m of measured photons [(a) $m=1$, (b) $m=2$, (c) $m=3$, (d) $m=4$].

$$c_{m,n}^{(\pm)}(\alpha)=\frac{(n+m)!}{\Gamma[(n+m)/2+1]\sqrt{n!}}\left(\pm\sqrt{\frac{1}{2}}\alpha\right)^{n+m}. \quad (39)$$

The normalization factor $\mathcal{N}_m^{(\pm)}$ is calculated to be [see Eqs. (B3) and (B11)]

$$\mathcal{N}_m^{(\pm)}=2\mathcal{N}_m-\frac{m!^2(-|\alpha|)^m}{\sqrt{\pi}2^m\Gamma(m+3/2)}$$

$$\times F[\tfrac{1}{2}(m+1),\tfrac{1}{2}(m+1),\tfrac{1}{2}(2m+3),1-\alpha^2],$$

$$(40)$$

$\mathcal{N}_m$ being given in Eq. (16). In Eq. (40), $F(\alpha,\beta,\gamma,z)$ is the hypergeometric function, and the normalization con-

stant A in Eq. (37) is simply given by $A=\tfrac{1}{2}(\mathcal{N}_m^{(\pm)}/\mathcal{N}_m)^{1/2}$. Note that $\mathcal{N}_m^{(\pm)}\approx2\mathcal{N}_m$, i.e., $A\approx1/\sqrt{2}$ for larger m (the approximation is very good for $m>4$).

Plots of the Wigner function of the states $|\Psi_m^{(+)}\rangle$ are given in Fig. 4. The behavior of the states $|\Psi_m^{(-)}\rangle$ is quite similar. From the figure we see that the states $|\Psi_m^{(+)}\rangle$ (and also the states $|\Psi_m^{(-)}\rangle$) are very close to squeezed coherent states. For chosen α the squeezing effect decreases with increasing m. The small deviation from Gaussian states is indicated by the negative values of the Wigner function (which in our case are of the order of magnitude of -10^{-5}). To illustrate the difference between the states $|\Psi_m^{(\pm)}\rangle$ and the squeezed coherent states, let us consider the Husimi function $Q^{(\pm)}(x,p|m)$ of $|\Psi_m^{(\pm)}\rangle$. According to Eq. (B13) we obtain
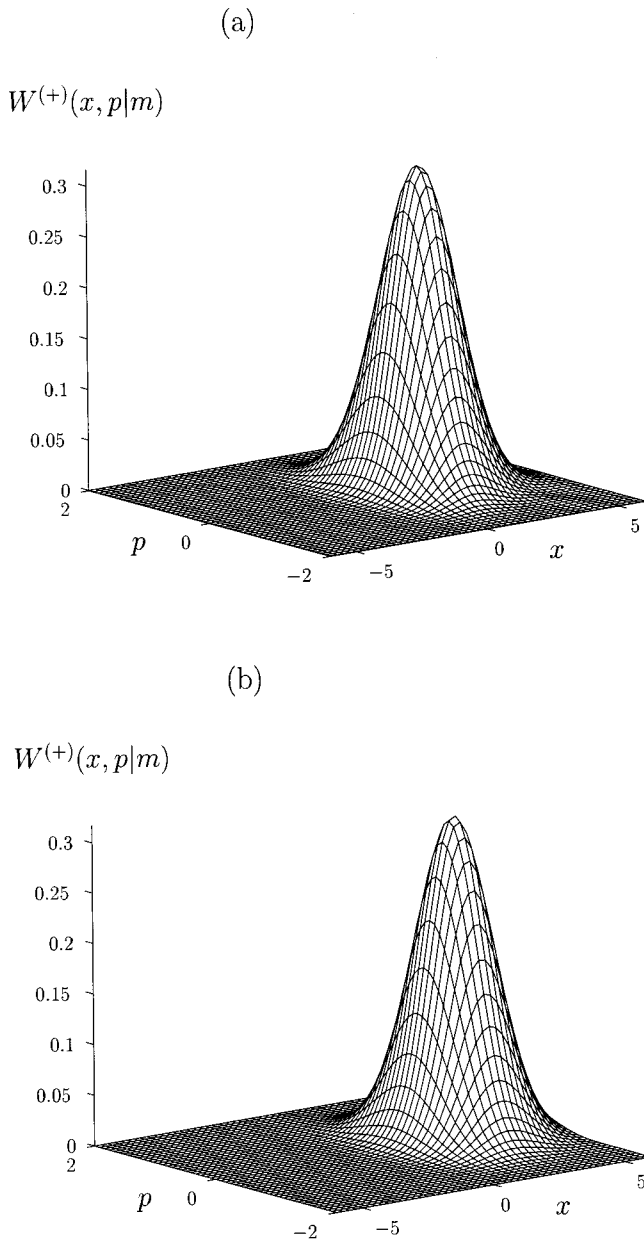
(a)

$W^{(+)}(x,p|m)$

(b)

$W^{(+)}(x,p|m)$

FIG. 4. Wigner function $W^{(+)}(x,p|m)$ of the state $|\Psi_m^{(+)}\rangle$ for $\alpha=0.6$ and various numbers m of measured photons [(a) $m=1$, (b) $m=3$].

$$Q^{(\pm)}(x,p|m)=\frac{\alpha^m(m!)^2}{\pi^2\mathcal{N}_m^{(\pm)}}e^{-|\beta|^2}\exp[\tfrac{1}{4}\alpha(\beta^2+\beta^{*2})]$$
$$\times|D_{-m-1}(\pm\sqrt{\alpha}\beta)|^2, \qquad (41)$$

where $\beta=(x+ip)/\sqrt{2}$, and $D_m(z)$ is the parabolic cylinder function (which indicates the deviation from a Gaussian). Recalling the asymptotic behavior of the $D_{-m-1}(z)$ for large values of m [26], we find that

$$Q^{(\pm)}(x,p|m)\propto\exp[-|\beta|^2\pm\sqrt{\alpha m}(\beta+\beta^*)-|\sqrt{\alpha m}|^2]$$
$$\qquad (42)$$

($m\rightarrow\infty$), which corresponds to the scalar product $|\langle\beta|\gamma\rangle|^2$ between the coherent states $|\beta\rangle$ and $|\gamma\rangle$, with $\gamma=\pm\sqrt{\alpha m}$. Thus for sufficiently large numbers of detected photons, m, the component states $|\Psi_m^{(\pm)}\rangle$ approach coherent states. This kind of behavior has also been found in Ref. [11] for the states studied therein.

IV. REALISTIC PHOTON COUNTING

In order to produce the conditional states $|\Psi_m\rangle$, highly efficient and precise photocounting is needed. Unfortunately, there have been no highly efficient photodetectors available which precisely distinguish between m and $m+1$ photons. Recently the proposal has been made to measure the photon-number statistics using photon chopping [25]. The mode to be detected is used as an input of an optical $2N$-port, the other input ports being unused. To each of the output ports a highly efficient avalanche photodiode is connected which can distinguish between photons being present or absent. The photon-number statistics of the input mode can then be obtained from the recorded output coincident-event statistics.

In particular, if m photons are present in the input, the probability of recording k coincident events is given by [25]

$$\widetilde{P}_N(k|m)=\frac{1}{N^m}\binom{N}{k}\sum_{l=0}^{k}(-1)^l\binom{k}{l}(k-l)^m \qquad (43)$$

for $k\leq m$, and $\widetilde{P}_N(k|m)=0$ for $k>m$. Note that $\widetilde{P}_N(k|m)\rightarrow\delta_{k,m}$ for $N\rightarrow\infty$. In Eq. (43) perfect detection is assumed. The effect of nonperfect detection corresponds to a random process such that photons are excluded from detection with probability $1-\eta$, η being the efficiency of the photodiodes ($0<\eta\leq1$). The probability of recording k coincident events then modifies to

$$\widetilde{P}_{N,\eta}(k|m)=\sum_l\widetilde{P}_N(k|l)M_{l,m}(\eta), \qquad (44)$$

where the matrix $M_{l,m}(\eta)$ is given by

$$M_{l,m}(\eta)=\binom{m}{l}\eta^l(1-\eta)^{m-l} \qquad (45)$$

for $l\leq m$, and $M_{l,m}(\eta)=0$ for $l>m$.

Since detection of k coincident events can result from various numbers m of photons, the conditional state is in general a statistical mixture. Therefore in place of Eq. (12) we now have

$$\hat{\varrho}_{\text{out}}(k)=\sum_m P_{N,\eta}(m|k)|\Psi_m\rangle\langle\Psi_m|, \qquad (46)$$

where $|\Psi_m\rangle$ is given in Eq. (13), and $P_{N,\eta}(m|k)$ is the probability of m photons being present under the condition that k coincidences are recorded. The conditional probability $P_{N,\eta}(m|k)$ can be obtained using the Bayes rule as

$$P_{N,\eta}(m|k)=\frac{1}{\widetilde{P}_{N,\eta}(k)}\widetilde{P}_{N,\eta}(k|m)P(m). \qquad (47)$$
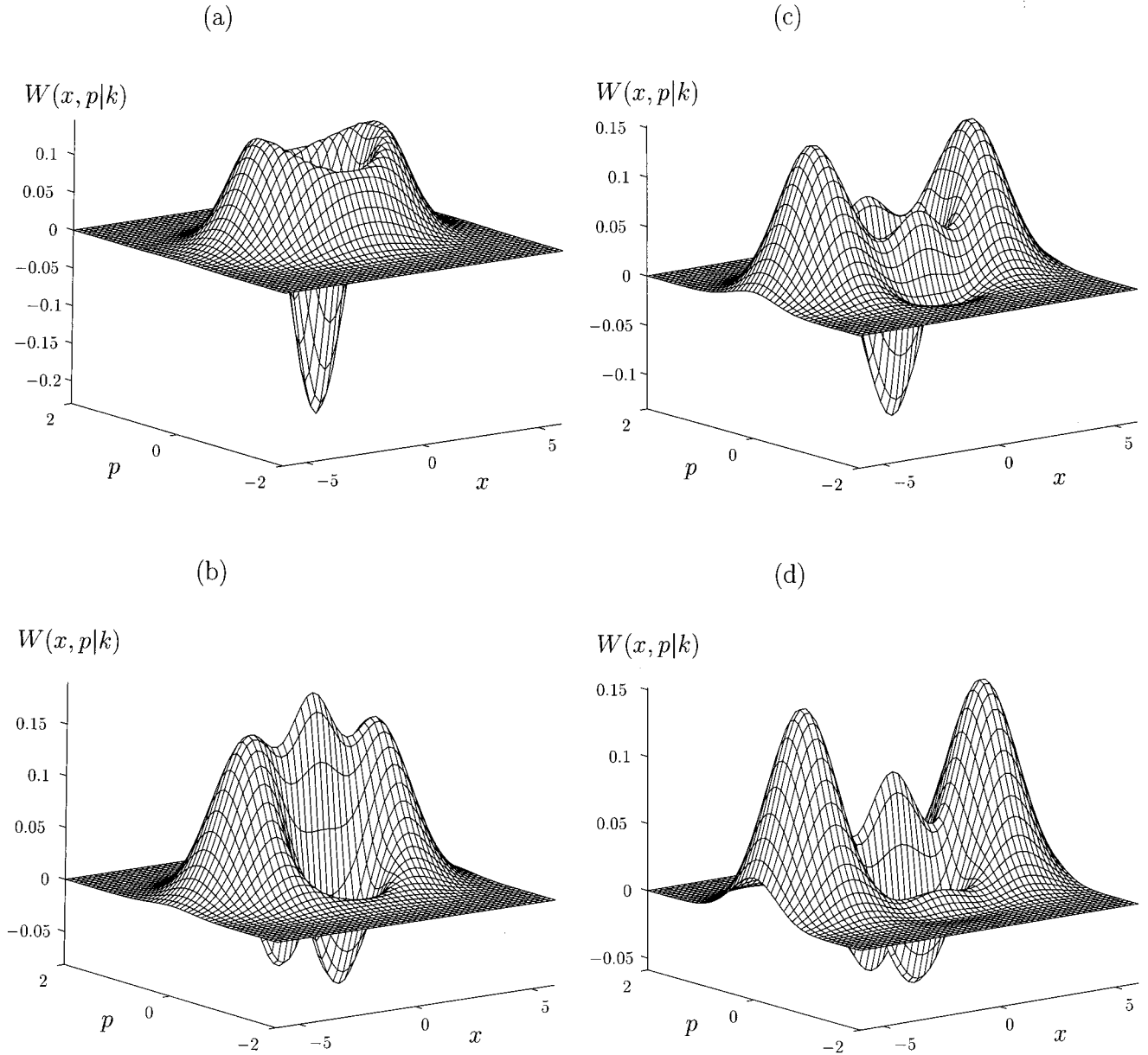
(a)

(c)

(b)

(d)

FIG. 5. Wigner function of the conditional state with realistic photodetection ($N=10$, $\eta=0.8$) for $\kappa=0.75$, $|T|^2=0.8$ ($\alpha=0.6$), and various numbers k of coincident events [(a) $k=1$, $\widetilde{P}_{N,\eta}(k)=10.99\%$; (b) $k=2$, $\widetilde{P}_{N,\eta}(k)=2.95\%$; (c) $k=3$, $\widetilde{P}_{N,\eta}(k)=0.69\%$; (d) $k=4$, $\widetilde{P}_{N,\eta}(k)=0.16\%$], the probabilities $\widetilde{P}_{N,\eta}(k)$ of the coincidences being calculated according to Eq. (48).

Here $P(m)$ is the prior probability (17) of m photons being present, and accordingly, $\widetilde{P}_{N,\eta}(k)$ is the prior probability of recording k coincident events,

$$\widetilde{P}_{N,\eta}(k) = \sum_m \widetilde{P}_{N,\eta}(k|m) P(m). \qquad (48)$$

Examples of the Wigner function and the quadrature-component distributions of the conditional (mixed) states (46) are plotted in Figs. 5 and 6, respectively. We see that the quantum interferences can still be preserved also for realistic values of the number of photodiodes and their efficiencies, such as $N=10$ and $\eta=80\%$. As expected, the probabilities of observing the conditional states, $\widetilde{P}_{N,\eta}(k)$, Eq. (48), decrease with increasing k (from about 11% for $k=1$ to

0.16% for $k=4$ in the case when $|T|^2=0.8$). Nevertheless, with a sufficiently high repetition frequency of the input states the method could assure a comparatively efficient source of the catlike states. The interference structure is (for chosen N and η) more and more smeared with increasing k. Clearly, a larger number of detected coincidences implies (for chosen N and η) a larger probability of "losing" some of the photons. Any lost photon switches the parity of the conditional state (from even to odd and vice versa) and therefore destroys the interference pattern.

V. CONCLUSION

We have shown that Schrödinger-cat-like states can be generated by conditional measurements using a simple beam splitter scheme. When a squeezed vacuum and an ordinary
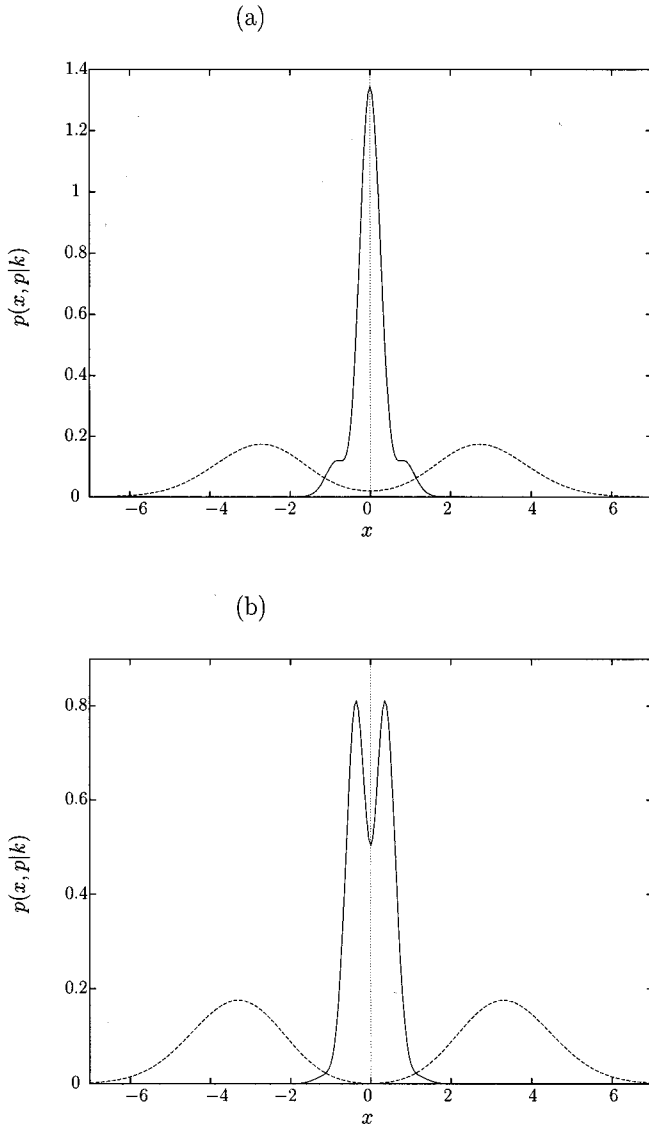
(a)

(b)

FIG. 6. Quadrature distribution of the conditional state with realistic photodetection ($N=10$, $\eta=0.8$) for the phase parameters $\varphi=0$ (full line) and $\varphi=\pi/2$ (broken line), various numbers k of coincident events [(a) $k=2$, (b) $k=3$], and $\kappa=0.75$, $|T|^2=0.8$ ($\alpha=0.6$).

vacuum are mixed by a beam splitter and the number of photons is measured in one of the output channels , then the conditional quantum state in the other output channel reveals all the properties of a Schrödinger-cat-like state.

To demonstrate this, we have analyzed the conditional states in terms of the photon-number and quadrature-component distributions and the Wigner and Husimi functions and have presented both analytical and numerical results. We have studied the component states and shown that they are very close to squeezed coherent states and approach coherent states for sufficiently large numbers of detected photons. We have found that the basic features of Schrödinger-cat-like states, such as the appearance of two separated peaks and the interference pattern, become more pronounced for larger values of the transmittance of the beam splitter, the squeezing parameter of the input state, and the number of detected photons. On the other hand, increas-

ing transmittance implies a decrease of the probability of photons being present, so that the ''better'' Schrödinger-cat-like states appear more rarely.

We have also discussed the problem of producing the Schrödinger-cat-like states under the conditions of realistic photocounting. For this purpose we have assumed multi-channel detection using highly efficient avalanche photodiodes. As expected, the measurement smears the interference structure. However, for properly chosen parameters the interference structure can still be found even for a realistic arrangement of detectors.

ACKNOWLEDGMENTS

APPENDIX A: SUM RULES

Using the expansion in the Fock basis of $|\Psi_m\rangle$, Eq. (13), various photon-number summations must be performed in the further calculations, which can be done advantageously by means of Hermite polynomials. For this purpose we rewrite the coefficients $c_{m_2,n_1}(\alpha)$, Eq. (14), as

$$c_{m_2,n_1}(\alpha)=\frac{[2(n+k+\delta)]!}{(n+k+\delta)!\sqrt{(2n+\delta)!}}(\tfrac{1}{2}\alpha)^{n+k+\delta}, \quad (A1)$$

where $\delta=0$ for $n_1=2n$ and $m_2=2k$, and $\delta=1$ if $n_1=2n+1$ and $m_2=2k+1$. Note that $c_{m_2,n_1}(\alpha)=0$ otherwise. Recalling the relation

$$H_{2n}(0)=(-1)^n(2n)!/n!, \quad (A2)$$

we see that

$$c_{m_2,n_1}(\alpha)=\frac{1}{\sqrt{(2n+\delta)!}}H_{2(n+k+\delta)}(0)(-\tfrac{1}{2}\alpha)^{n+k+\delta}. \quad (A3)$$

This enables us to apply standard summation rules, such as Mehler's formula [26]

$$\sum_{k=0}^{\infty}\frac{1}{k!}H_k(x)H_k(y)(\tfrac{1}{2}z)^k=\frac{1}{\sqrt{1-z^2}}$$
$$\times\exp\left[\frac{2xyz-(x^2+y^2)z^2}{1-z^2}\right]. \quad (A4)$$

Taking the lth and jth derivatives with respect to x and y, respectively, of both sides of this equation and using the relation

$$\frac{d^j}{dx^j}H_k(x)=2^j\frac{k!}{(k-j)!}H_{k-j}(x), \quad (A5)$$

we derive that

$$\sum_{k=0}^{\infty}\frac{1}{k!}H_{k+l}(x)H_{k+j}(y)(\tfrac{1}{2}z)^k$$

$$=\frac{1}{(1-z^2)^{(l+j+1)/2}}\exp\left[\frac{2xyz-(x^2+y^2)z^2}{1-z^2}\right]$$

$$\times\sum_{k=0}^{\min(l,j)}\binom{l}{k}\binom{j}{k}(2z)^k k!H_{l-k}\left(\frac{x-zy}{\sqrt{1-z^2}}\right)H_{j-k}\left(\frac{y-zx}{\sqrt{1-z^2}}\right).$$
$$(A6)$$

Another useful sum rule is

$$\sum_{k=0}^{\infty}\frac{1}{k!}H_{k+j}(x)(\tfrac{1}{2}z)^k=\exp(xz-\tfrac{1}{4}z^2)H_{k+j}(x-\tfrac{1}{2}z),$$
$$(A7)$$

which may be derived by taking the jth derivative of the generating function of the Hermite polynomials,

$$\sum_{k=0}^{\infty}H_k(x)\frac{z^k}{k!}=\exp(2xz-z^2).\qquad(A8)$$

APPENDIX B: DERIVATION OF THE RELATIONS (40) AND (41)

From Eqs. (13), (14), and (37)–(39) we see that

$$c_{m,n}(\alpha)=\frac{1}{2}[c_{m,n}^{(+)}(\alpha)+c_{m,n}^{(-)}(\alpha)],\qquad(B1)$$

and hence

$$\sum_{n=0}^{\infty}|c_{m,n}(\alpha)|^2=\frac{1}{4}\left\{\sum_{n=0}^{\infty}|c_{m,n}^{(+)}(\alpha)|^2+\sum_{n=0}^{\infty}|c_{m,n}^{(-)}(\alpha)|^2\right.$$

$$\left.+2\mathrm{Re}\left[\sum_{n=0}^{\infty}c_{m,n}^{(+)}(\alpha)c_{m,n}^{(-)}(\alpha)\right]\right\}.\qquad(B2)$$

Thus,

$$\mathcal{N}_m^{(\pm)}=\sum_{n=0}^{\infty}|c_{m,n}^{(\pm)}(\alpha)|^2=2\mathcal{N}_m-\mathcal{I}_m,\qquad(B3)$$

where $\mathcal{N}_m$ is given in Eq. (16), and

$$\mathcal{I}_m=\sum_{n=0}^{\infty}(-1)^{n+m}|c_{m,n}^{(\pm)}(\alpha)|^2.\qquad(B4)$$

Combining Eqs. (B4) and (39) yields

$$\mathcal{I}_m=\sum_{n=0}^{\infty}\frac{\Gamma^2(m+n+1)}{\Gamma^2[(m+n+2)/2]n!}(-\tfrac{1}{2}|\alpha|)^{n+m}.\qquad(B5)$$

Using the relation

$$\frac{\Gamma(2n)}{\Gamma(n+1/2)}=\frac{4^n}{2\sqrt{\pi}}\Gamma(n),\qquad(B6)$$

from Eq. (B5) we obtain

$$\mathcal{I}_m=\frac{1}{\pi}\sum_{n=0}^{\infty}\Gamma^2[\tfrac{1}{2}(m+n+1)]\frac{(-2|\alpha|)^{n+m}}{n!}.\qquad(B7)$$

Substituting in Eq. (B7) for the Γ function the integral representation, we may write

$$\mathcal{I}_m=\frac{(-2|\alpha|)^m}{\pi}\int_0^{\infty}dt_1\int_0^{\infty}dt_2\left[e^{-t_1}e^{-t_2}(t_1t_2)^{(m-1)/2}\right.$$

$$\left.\times\sum_{n=0}^{\infty}\frac{(-2|\alpha|\sqrt{t_1t_2})^n}{n!}\right],\qquad(B8)$$

which reduces to

$$\mathcal{I}_m=\frac{(-2|\alpha|)^m}{\pi}\int_0^{\infty}dt_1\left[e^{-t_1}(t_1)^{(m-1)/2}\right.$$

$$\left.\times\int_0^{\infty}dt_2 e^{-t_2}(t_2)^{(m-1)/2}e^{-2|\alpha|\sqrt{t_1t_2}}\right].\qquad(B9)$$

We first calculate the t_2 integral [26] to obtain

$$\mathcal{I}_m=\frac{m!(-\sqrt{2}|\alpha|)^m}{\pi}\times\int_0^{\infty}dt_1 2^{-(1-\alpha^2t_1/2)t_1}(t_1)^{(m-1)/2}$$

$$\times D_{-m-1}(\sqrt{2\alpha^2 t_1}).\qquad(B10)$$

Calculating the resulting t_1 integral [26], we eventually obtain

$$\mathcal{I}_m=\frac{m!^2(-|\alpha|)^m}{\sqrt{\pi}2^m\Gamma(m+3/2)}$$

$$\times F[\tfrac{1}{2}(m+1),\tfrac{1}{2}(m+1),m+\tfrac{3}{2},1-\alpha^2],\qquad(B11)$$

where $F(\alpha,\beta,\gamma,z)$ is the hypergeometric function.

The calculation of $\langle\Psi_m^{(\pm)}|\beta\rangle$ can be performed in a similar way. Using Eqs. (13), (14), (35), and (B6), we have

$$\langle\Psi_m^{(\pm)}|\beta\rangle=(\pm 1)^m\sqrt{\frac{(2\alpha)^m}{\pi\mathcal{N}_m^{(\pm)}}}e^{-|\beta|^2/2}$$

$$\times\sum_{n=0}^{\infty}\frac{(\pm\sqrt{2\alpha}\beta)^n}{n!}\Gamma[\tfrac{1}{2}(n+m+1)].$$
$$(B12)$$

Substituting in Eq. (B12) the integral representation for the Γ function again, we arrive at an integral of the type of the t_2 integral in Eq. (B9), which may be calculated using standard formulas [26]. We then obtain

$$\langle\Psi_m^{(\pm)}|\beta\rangle=(\pm 1)^m m!\sqrt{\frac{2\alpha^m}{\pi\mathcal{N}_m^{(\pm)}}}$$

$$\times e^{-|\beta|^2/2+\beta^2\alpha/4}D_{-m-1}(\pm\sqrt{\alpha}\beta),\qquad(B13)$$

where $D_m(z)$ is the parabolic cylinder function.

[1] E. Schrödinger, Naturwissenschaften **23**, 807 (1935); **23**, 823 (1935); **23**, 844 (1935).

[2] B. Yurke and D. Stoler, Phys. Rev. Lett. **57**, 13 (1986).

[3] J. Janszky, A.V. Vinogradov, T. Kobayashi, and Z. Kis, Phys. Rev. A **50**, 1777 (1994).

[4] I.A. Walmsley and M.G. Raymer, Phys. Rev. A **52**, 681 (1995).

[5] R.L. de Matos Filho and W. Vogel, Phys. Rev. Lett. **76**, 608 (1996).

[6] C. Monroe, D.M. Meekhof, B.E. King, and D.J. Wineland, Science **272**, 1131 (1996).

[7] M.M. Nieto, Phys. Lett. A **219**, 180 (1996).

[8] V. Bužek and P. L. Knight, in *Progress in Optics XXXIV*, edited by E. Wolf (North-Holland, Amsterdam, 1995).

[9] A. La Porta, R. E. Slusher, and B. Yurke, Phys. Rev. Lett. **62**, 28 (1989).

[10] S. Song, C. M. Caves, and B. Yurke, Phys. Rev. A **41**, 5261 (1990).

[11] B. Yurke, W. Schleich, and D. F. Walls, Phys. Rev. A **42**, 1703 (1990).

[12] P. Tombesi and D. Vitali, Phys. Rev. Lett. **77**, 411 (1996).

[13] P. Goetsch, P. Tombesi, and D. Vitali, Phys. Rev. A **54**, 4519 (1996).

[14] M. Ban, Phys. Rev. A **49**, 5078 (1994).

[15] M. Ban, J. Mod. Opt. **43**, 1281 (1996).

[16] B. Yurke, S.L. McCall, and J.R. Klauder, Phys. Rev. A **33**, 4033 (1986).

[17] R.A. Campos, B.E.A. Saleh, and M.C. Teich, Phys. Rev. A **40**, 1371 (1989).

[18] L. Mandel, Opt. Lett. **4**, 205 (1979).

[19] W. Vogel and D.-G. Welsch, *Lectures on Quantum Optics* (Akademie Verlag, Berlin, 1994).

[20] I.S. Gradshteyn and I.M. Ryzhik, *Tables of Integrals, Series and Products* (Academic, New York, 1980).

[21] N.G. Walker, J. Mod. Opt. **34**, 15 (1987).

[22] A. Zucchetti, W. Vogel, and D.-G. Welsch, Phys. Rev. A **54**, 856 (1996).

[23] N.G. Walker and J.E. Caroll, Electron. Lett. **20**, 981 (1984).

[24] M. Freyberger, K. Vogel, and W.P. Schleich, Phys. Lett. A **176**, 41 (1993).

[25] H. Paul, P. Törmä, T. Kiss, and I. Jex, Phys. Rev. Lett. **76**, 2464 (1996).

[26] A. Erdelyi, *Higher Transcendental Functions*, Batman Manuscript Project, Vol. 3 (McGraw-Hill, New York, 1953).